PHILOSOPHICAL TRANSACTIONS A

rsta.royalsocietypublishing.org

Research

Cite this article: Borg M, Collu M. 2015 A comparison between the dynamics of horizontal and vertical axis offshore floating wind turbines. *Phil. Trans. R. Soc. A* **373**: 20140076.
http://dx.doi.org/10.1098/rsta.2014.0076

One contribution of 17 to a theme issue 'New perspectives in offshore wind energy'.

Subject Areas:
energy, mechanical engineering, ocean engineering, mathematical modelling

Keywords:
renewable energy, offshore wind, floating wind turbines, vertical axis wind turbine, horizontal axis wind turbine, dynamics

Author for correspondence:
M. Collu
e-mail: maurizio.collu@cranfield.ac.uk

A comparison between the dynamics of horizontal and vertical axis offshore floating wind turbines

M. Borg and M. Collu

Offshore and Renewable Energy, Cranfield University, Cranfield MK43 0AL, UK

MB, 0000-0001-8438-2306; MC, 0000-0001-7692-4988

The need to further exploit offshore wind resources in deeper waters has led to a re-emerging interest in vertical axis wind turbines (VAWTs) for floating foundation applications. However, there has been little effort to systematically compare VAWTs to the more conventional horizontal axis wind turbine (HAWT). This article initiates this comparison based on prime principles, focusing on the turbine aerodynamic forces and their impact on the floating wind turbine static and dynamic responses. VAWTs generate substantially different aerodynamic forces on the support structure, in particular, a potentially lower inclining moment and a substantially higher torque than HAWTs. Considering the static stability requirements, the advantages of a lower inclining moment, a lower wind turbine mass and a lower centre of gravity are illustrated, all of which are exploitable to have a less costly support structure. Floating VAWTs experience increased motion in the frequency range surrounding the turbine [number of blades] × [rotational speed] frequency. For very large VAWTs with slower rotational speeds, this frequency range may significantly overlap with the range of wave excitation forces. Quantitative considerations are undertaken comparing the reference NREL 5 MW HAWT with the NOVA 5 MW VAWT.

1. Introduction

The need to further exploit offshore wind resources has pushed offshore wind turbines into deeper waters, where floating support foundations become more economically viable than fixed support foundations [1]. The recent

THE ROYAL SOCIETY PUBLISHING

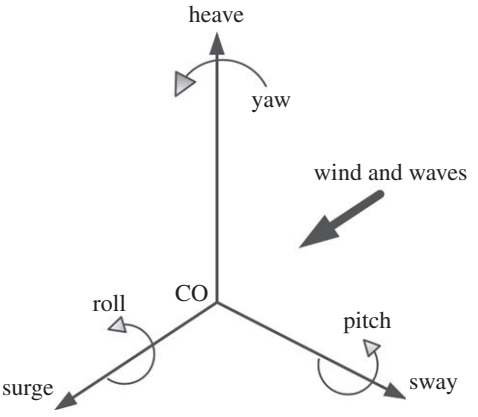

Figure 1. Definition of coordinate system.

re-emerging interest in vertical axis wind turbines (VAWTs) for floating foundation applications has resulted in a number of studies being performed for this class of turbine by different researchers [2].

Here, the comparison focus is on the substantial difference of the aerodynamic forces generated by horizontal axis wind turbine (HAWT) and VAWT systems, and their impact on the static and dynamic responses of the floating wind turbine systems.

(a) Previous floating vertical axis wind turbine research

While there is a substantial body of work on the dynamics of floating HAWTs, there have been relatively few studies that have focused on the dynamics of floating VAWTs. Vita [3] analysed a Darrieus-type rotor installed on a surface piercing articulated reservoir (SPAR) buoy rotating platform at a technical and economic level. Collu *et al.* [4] presented the preliminary design and optimization of a floating support structure for the NOVA rotor. The concept of this novel vertical axis rotor is to reduce the overturning moment acting on the support structure while maintaining sufficient power output. Another concept was proposed by Akimoto *et al.* [5] for a 'floating axis' wind turbine. This concept differs from that proposed by Vita because the generator is located outside the floating platform, with roller bearings transferring torque from the rotating tower to generators around the tower. Another concept, VertiWind, was proposed by Cahay *et al.* [6] for a three-bladed H-type Darrieus rotor mounted on a semi-submersible similar to the Dutch tri-floater design.

(b) Coordinate system definition

A floating wind turbine undergoes six d.f. motion, namely three translation motions (surge, sway and heave) and three rotational motions (roll, pitch and yaw). These d.f. are depicted in figure 1 in relation to the incident wind and wave direction. The origin of the coordinate system, CO, is usually located on the mean sea level at the centre of flotation, which is defined in §2*b*(i).

2. Some considerations on floating wind turbine systems based on prime principles

(a) Aerodynamic loads

(i) Fundamentals of wind turbine aerodynamics

The purpose of a wind turbine is to extract kinetic energy from the wind flowing through it. The earliest aerodynamic model for a wind turbine is generally attributed to Betz [7], based

on one-dimensional momentum flow theory developed by Rankine [8] and Froude [9]. This model consists of representing the wind turbine as a permeable actuator disc through which the flow of fluid experiences a loss of energy. The resulting reduction in fluid flow velocity and pressure drop, Δp, downwind of the actuator disc results in a thrust force, T, acting on the actuator disc

$$T = \Delta p \cdot A, \tag{2.1}$$

where A is the area of the disc. Through the application of the Bernoulli, mass conservation and momentum conservation equations, (2.1) is transformed into

$$T = 2\rho A V_\infty^2 a(1-a), \tag{2.2}$$

where ρ is the fluid density, V_∞ is the free-stream velocity and a is the axial induction factor that relates the free-stream velocity to the fluid velocity passing through the actuator disc. An equivalent drag or thrust coefficient, C_T, can be defined as

$$C_T = \frac{T}{(1/2)\rho A V_\infty^2} = 4a(1-a). \tag{2.3}$$

Furthermore, the power extracted by the actuator disc from the fluid is given by

$$P = T.V_\infty = 2\rho A V_\infty^3 a(1-a)^2. \tag{2.4}$$

The above is then integrated differently with blade element theory to predict blade and rotor forces for HAWTs and VAWTs. The different approaches used are summarized below.

(ii) Horizontal axis wind turbine momentum model

First formulated by Glauert [10] in the investigation of propellers, blade element theory involves the discretization of the blades into a number of aerodynamically independent elements that are treated as two-dimensional aerofoils. Local aerodynamic blade forces can be found based on local flow conditions, and the global aerodynamic forces are found through the integral of local blade forces along all blade lengths. Coupling this theory with the momentum flow theory by assuming the loss of momentum/pressure across the turbine equals the work done on the blade elements by the fluid flowing through the turbine, the retardation of the wind through the rotor may be obtained. Subsequent work expands on this to consider a number of different aspects and corrections related to HAWTs, including dynamic stall, tip and hub losses, high loading and skewed wake [11].

(iii) Vertical axis wind turbine momentum model

A number of increasingly detailed momentum models for VAWTs have been developed over the years [12–14], with the most elaborate variant formulated by Paraschiviou [15] and known as the double-multiple streamtube model. Briefly, the VAWT is decomposed into two regions: the upwind half-cycle and the downwind half-cycle and are mathematically represented as tandem actuator discs. Furthermore, each region is divided horizontally and vertically into a number of aerodynamically independent streamtubes. By applying blade element momentum theory to each streamtube, the induction factors as a function of azimuthal position, and subsequently local blade forces, can be evaluated.

(iv) Typical rotor loads

The aerodynamic forces produced by HAWTs and VAWTs are markedly different in all six d.f. For identical steady wind conditions, VAWT aerodynamic forces are highly oscillatory while HAWT

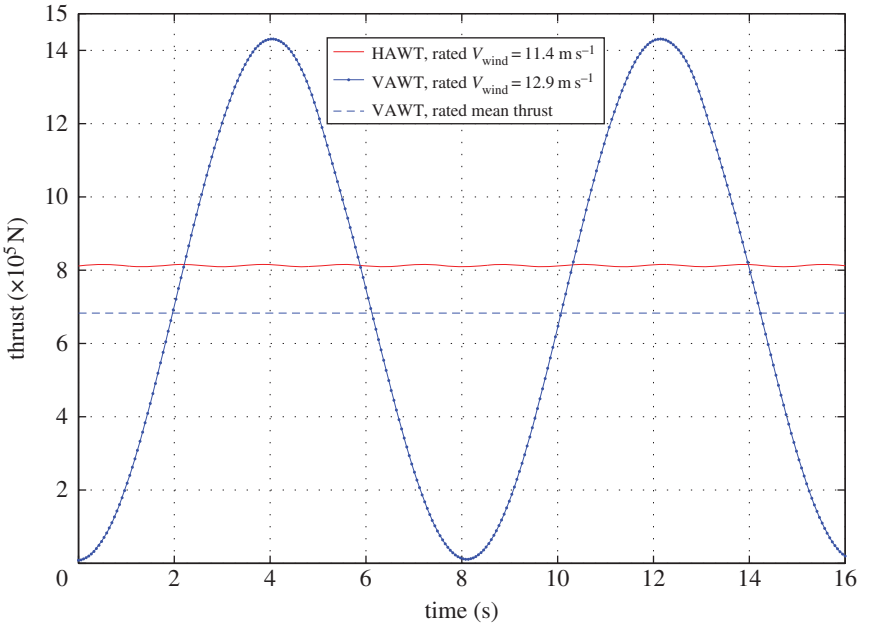

Figure 2. VAWT and HAWT rotor thrust forces at rated wind speeds obtained using FloVAWT [18] and FAST [17], respectively. (Online version in colour.)

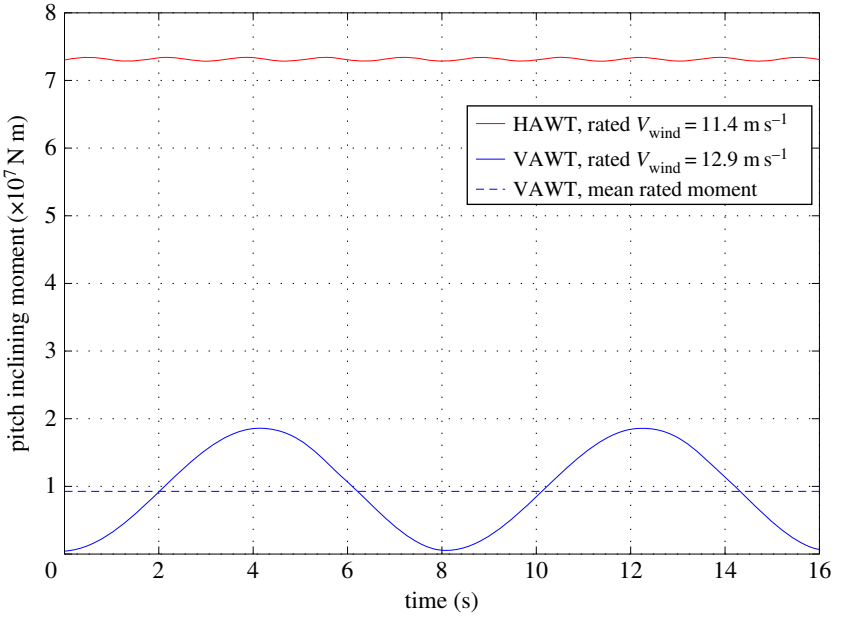

Figure 3. VAWT and HAWT rotor inclining moments at rated wind speeds obtained using FloVAWT [18] and FAST [17], respectively. (Online version in colour.)

aerodynamic forces are fairly constant. To illustrate this difference, sample time series of the rotor thrust forces generated by the NREL 5 MW reference HAWT [16] and the NOVA 5 MW VAWT [17] at the respective rated wind speeds are presented in figures 2 and 3.

While the HAWT thrust forces contain small oscillations at the $(n \cdot p)_{\mathrm{HAWT}}$ frequency (n = number of blades, p = rotation frequency), the VAWT thrust forces vary from approximately zero

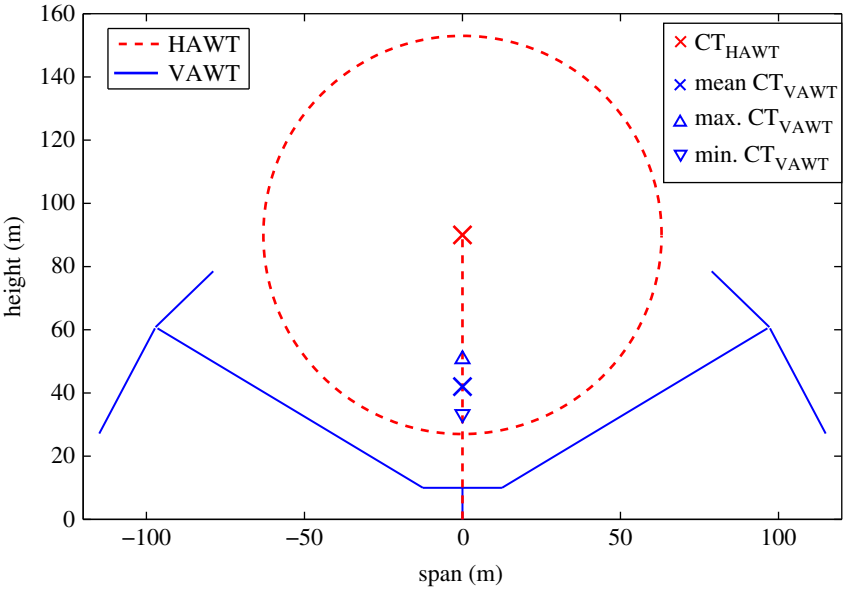

Figure 4. Front view schematic of HAWT and VAWT, with the centre of thrust pressure, C_T, indicated. Note that the height of the VAWT C_T varies as the turbine rotates, with maximum and minimum values indicated. (Online version in colour.)

to maximum at a frequency equal to the $(n \cdot p)_{VAWT}$ frequency. These trends are also present for the aerodynamic pitch inclining moments and shaft torque. As highlighted by figure 3 there is a substantial difference in the inclining moments, which is due to the much lower line of action of the VAWT as compared to the HAWT (illustrated in figure 4).

Another significant difference between HAWTs and VAWTs is that VAWTs generate significant oscillatory aerodynamic forces in all six d.f. while HAWTs generate relatively steady aerodynamic forces in d.f. relating to thrust, pitch overturning moment and roll overturning moment. This aspect is of particular importance to floating wind turbines as it may have a significant impact on the design, cost and feasibility of such devices, as will be further elaborated in §3.

(b) Static stability

The basic theory of hydrostatics of floating bodies is well known (e.g. [19]). It is, however, appropriate to start from the prime principles and apply them to the specific case of a floating offshore wind turbine (FOWT).

In general, for a partially submerged body of arbitrary shape, subject to arbitrary large inclination angles, it is necessary to adopt a fundamental approach, which is the integration of the pressure distribution on the submerged area, in order to estimate all the necessary hydrostatic characteristics.

However, in order to develop a deeper understanding of the static stability of floating wind turbine systems, the following simplifying hypotheses are considered in the present work: the fluid in which the body is immersed is at rest, the body is always in equilibrium and therefore the amount of submerged volume is constant during the (quasi-static) rotation, and the angle of inclination of the body is small (small angle approximation). This is usually called 'initial stability' analysis. The analysis will also be restricted to the pitch rotational d.f. (rotation about the y axis), but can be easily extended to roll rotational displacements.

(i) Reference points

Given the floating body in figure 5, the following definitions are given:

— *Axis system*. An orthogonal axis system is defined, with x aligned with the direction of the wind, z perpendicular to x and vertical upward and the origin coincident with F (therefore $z = 0$ at waterline level).
— *Centre of buoyancy* (B). The geometric centroid of the submerged volume of a body through which the total buoyancy may be assumed to act.
— *Centre of flotation* (F). The geometric centroid of the area of the waterplane of any waterline. A waterline is the intersection line of the free water surface with the moulded surface of the body.
— *Centre of gravity* (G). The centre through which all the weights constituting the system may be assumed to act.
— *Centre of mooring line action* (MLA). The intersection of the line of action of the horizontal component of the mooring force with the z axis is defined as the reference point of the mooring line action.
— *Centre of pressure of environmental forces* (CP(env)). The environmental forces acting on the FOWT system will be: aerodynamic forces, hydrodynamic forces and current forces. If an equilibrium state is considered (no waves, only constant wind and current forces), the centre of pressure of environmental forces is defined as the point on which the sum of the environmental forces (F_{env}) act.

(ii) Inclining moment

Referring to figure 5, the sum of the environmental forces F_{env} is counteracted by the horizontal component of the mooring system force ($F = F_{\mathrm{env}}$). The inclining moment (in the x–z plane) M_{I} is the moment resulting from these two forces, and can be estimated as F_{env} multiplied by the vertical distance between CP(env) and the point where F_{env} is counteracted, C_{MLA}, or

$$M_{\mathrm{I}} = F_{\mathrm{env}} \cdot (z_{\mathrm{CP(env)}} - z_{\mathrm{MLA}}) \cos\theta. \tag{2.5}$$

(iii) Restoring moment

The moments counteracting the inclining moment, whose sum is the restoring moment, can depend on three system characteristics: geometrical, inertial (mass and G) and in the case of tensioned mooring systems (e.g. tension leg platform (TLP)), the mooring system. The initial position of B and the second moment of the waterplane area (linked to the movement of B when the platform is inclined) are the characteristics determining the geometric contribution to the restoring moment.

For freely floating bodies (such as ships), where F_{B} is equal to mg, all the contributions are summarized in the parameter called the metacentric height, GM (see equation (2.14)).

For an offshore floating wind turbine, F_{B} can be higher than mg, due to the downward force of the mooring system. It is then preferred to classify the stabilization mechanisms in: a term taking into account the waterplane area contribution (geometric), a term taking into account the G position and the *initial* B position (geometric-inertial) and a term related to the (possible) contribution of the mooring system (mooring). In the following, this last approach is illustrated, and the equivalence with the classic approach is demonstrated for the particular case of freely floating bodies (equation (2.14)).

Restoring moment due to the waterplane area. If a rotation around the y-axis is imposed on the body, part of the initial waterplane area where x is positive will be submerged, while the part where x is negative will emerge. This means that on the first side there will be an additional submerged volume, while on the other side there will be an equal (in quantity) amount of volume

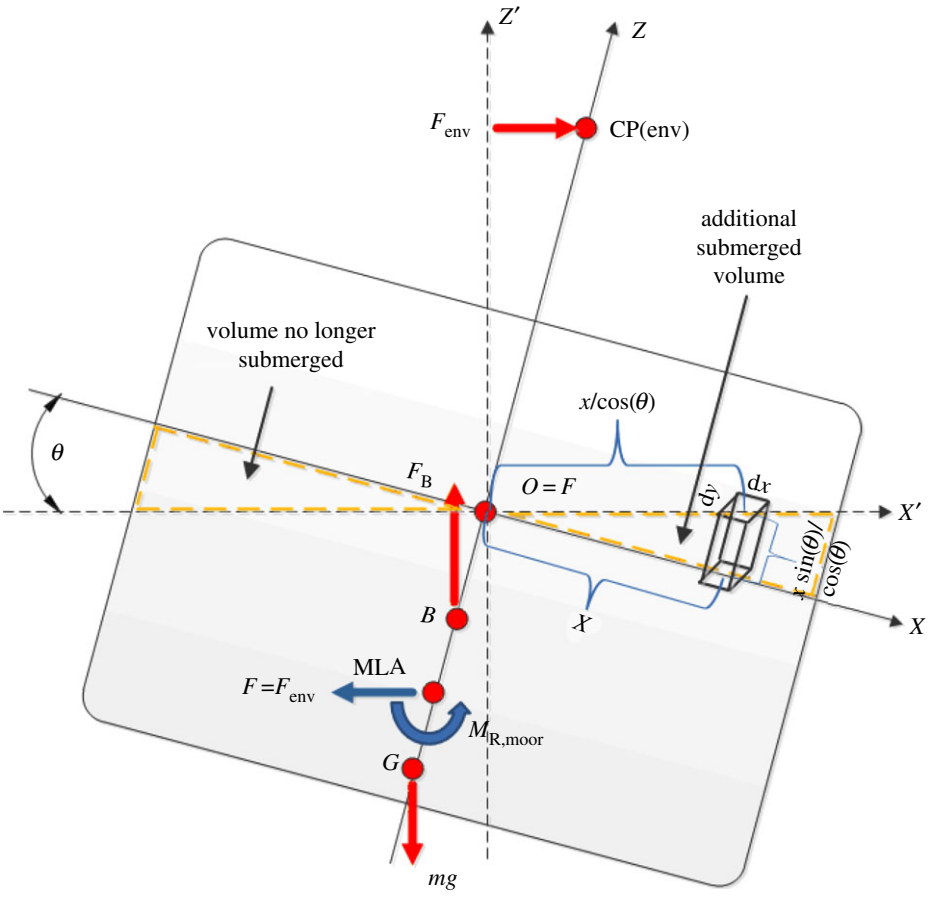

Figure 5. Diagram of forces and moments acting on a floating wind turbine system, longitudinal plane (pitch degree of freedom). (Online version in colour.)

no longer submerged. This will create a restoring couple that can be estimated by integrating the contribution of the change of submerged volume over the waterplane area (figure 5)

$$M_{R,WP} = \rho g \int\int \frac{x}{\cos\theta} \cdot \sin\theta \cdot x \, dx \, dy = \rho g \frac{\sin\theta}{\cos\theta} \int\int x^2 \, dx \, dy = \rho g I_x \frac{\sin\theta}{\cos\theta}, \tag{2.6}$$

where I_x is the second moment of area of the initial waterplane area (within the approximation of small inclination, the waterplane area does not change) with respect to the x axis.

Restoring moment due to B and G positions. Since the change of submerged volume and, consequently, the change of position of B is taken into account through equation (2.6), B can be considered fixed in the initial position for this approach, and the moments generated with respect to the origin by the buoyancy force, F_B, and the weight force, F_W, can be taken into account separately through

$$M_{R,G} = F_B \cdot z_B \cdot \sin\theta - m \cdot g \cdot z_G \cdot \sin\theta. \tag{2.7}$$

Restoring moment due to the mooring system. There are several mooring systems that have been adopted by the offshore floating wind industry. In general, its contribution to the total stiffness of the FOWT system may be represented by a 6 × 6 matrix, as it can generate counteracting forces in all d.f., and there can be coupled terms. For the present 1 d.f. analysis, it is assumed that the restoring moment in pitch is only proportional to the rotational displacement in pitch (decoupled from the other d.f.) and can be estimated as

$$M_{R,moor} = C_{55,moor} \cdot \theta. \tag{2.8}$$

Total restoring moment in pitch. Considering the three contributions to the restoring moment in equations (2.6)–(2.8), the total restoring moment is

$$M_{\mathrm{R}} = M_{\mathrm{R,WP}} + M_{\mathrm{R,CG}} + M_{\mathrm{R,moor}} \tag{2.9}$$

$$= \rho g I_x \frac{\sin\theta}{\cos\theta} + F_{\mathrm{B}} \cdot z_{\mathrm{CB}} \cdot \sin\theta - m \cdot g \cdot z_{\mathrm{CG}} \cdot \sin\theta + C_{55,\mathrm{moor}} \cdot \theta. \tag{2.10}$$

If the small angle of inclination approximation is adopted, $\sin\theta \simeq \theta$ and $\cos\theta \simeq 1$, and from equation (2.10), the total stiffness in pitch C_{55} can be defined as

$$M_{\mathrm{R}} = \rho g I_x \theta + F_{\mathrm{B}} \cdot z_{\mathrm{CB}} \cdot \theta - m \cdot g \cdot z_{\mathrm{CG}} \cdot \theta + C_{55,\mathrm{moor}} \cdot \theta \tag{2.11}$$

$$= (\rho g I_x + F_{\mathrm{B}} \cdot z_{\mathrm{CB}} - m \cdot g \cdot z_{\mathrm{CG}} + C_{55,\mathrm{moor}})\theta = C_{55} \cdot \theta. \tag{2.12}$$

Freely floating body case. If the body is freely floating and the contribution of the mooring system to the restoring force can be considered negligible, $F_{\mathrm{B}} = m \cdot g$, and (2.12) can be simplified to

$$M_R = \rho g I_x \theta + \rho \nabla g \left(\frac{I_x}{\nabla} + z_{\mathrm{CB}} - z_{\mathrm{CG}} \right) \sin\theta \tag{2.13}$$

$$= \rho \nabla g \left(\underbrace{\mathrm{BM} + z_{\mathrm{CB}}}_{\text{geometry}} - \underbrace{z_{\mathrm{CG}}}_{\text{weight}} \right) \sin\theta = \rho \nabla g \cdot \mathrm{GM} \sin\theta, \tag{2.14}$$

where GM is the longitudinal metacentric height, or distance between CG and M, the metacentre. If GM is positive, i.e. M above CG, then the floating body is stable.

N.B. Mooring system contributing both to inclining and restoring moment. Keeping in mind that the pitch d.f. is analysed here, the mooring system is contributing to the inclining moment through the horizontal force equal to F_{env}, but (in the case of tensioned mooring platform) can also contribute to the restoring moment through a restoring couple (e.g. for a TLP system, the difference between the vertical components of the tension in the cables provides a restoring moment).

(iv) Static stability requirement and classification of floating offshore wind turbine

Maximum angle of inclination and minimum stiffness. The aerodynamic performance of floating HAWT and VAWT systems operating with their axes of rotation not parallel (HAWT) or perpendicular (VAWT) to the wind direction is still a relatively unexplored research field [20–23]. According to Zambrano [23], a maximum mean pitch/roll angle of 5° combined with ±15° of dynamic amplitude should be imposed, in order not to substantially compromise the performance of the wind turbine, but it is only a guideline. In any case, it is clear that a maximum angle ($\theta_{\max}$) of inclination should be imposed in the design phase as one of the requirements for the floating support structure or, given an inclining moment, a minimum total stiffness should be provided by the floating support structure. According to equation (2.12), the minimum total stiffness is

$$C_{55,\min} = \frac{M_{\mathrm{I}}}{\theta_{\max}}. \tag{2.15}$$

Classification based on main stability mechanism. Referring to (2.10), the mechanism through which a FOWT system fulfils condition (2.15) is often used to classify FOWT systems [24]. The system is defined as waterplane-stabilized if the main contribution to the total M_{R} is $M_{\mathrm{R,WP}}$ (e.g. Dutch Trifloater [25], WindFloat [26], NOVA semi-submersible [4]), as ballast-stabilized if the main contribution is given by $M_{\mathrm{R,CG}}$ (e.g. Hywind SPAR by Statoil [27]), or as mooring-stabilized if

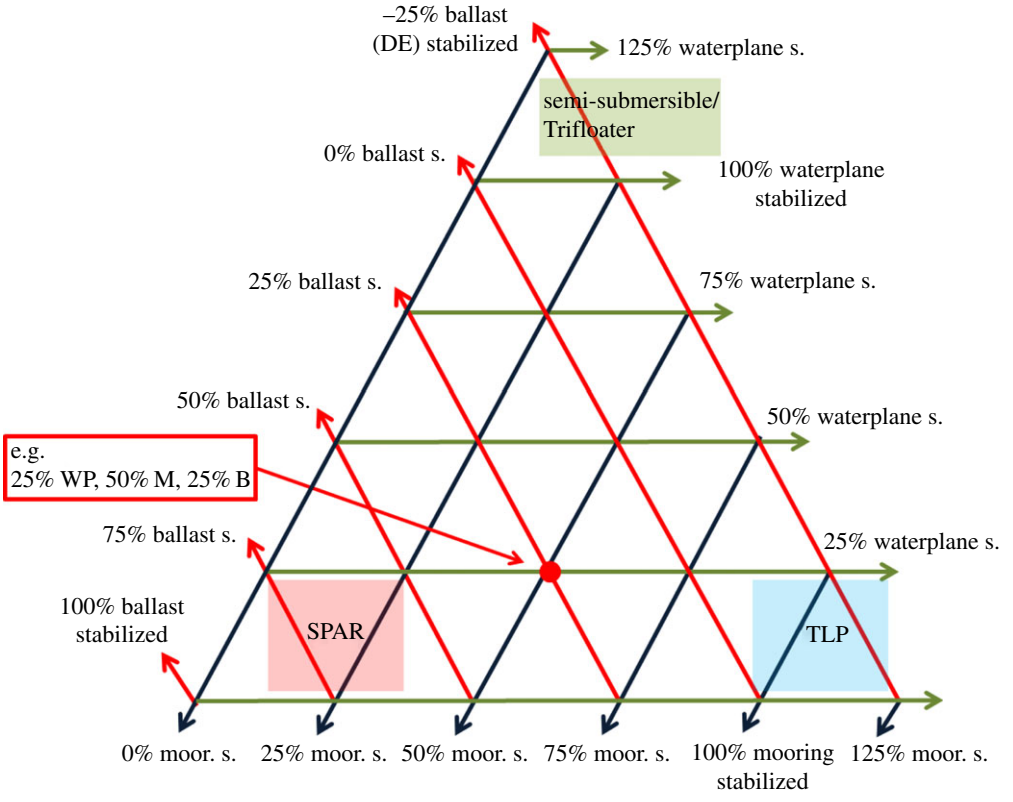

Figure 6. Stability triangle. The three corners of the triangle represent the three stabilization mechanisms exploited by floating wind turbine systems (see §2*b*(iii),(iv)). (Online version in colour.)

the main contribution comes from $M_{R,moor}$ (e.g. MIT TLP [24], BlueH by BlueH [28]). This is usually represented by the 'stability triangle', where the sum of the three contributions (each one going from contributing 0 to 100% of the total stiffness) amounts to the total stiffness of the system [24].

It is important to note that usually the contribution of the CG position is represented as positive or zero, while this is valid only if

$$F_B \cdot z_{CB} - m \cdot g \cdot z_{CG} \geq 0, \quad z_{CG} \leq \frac{F_B}{m \cdot g} z_{CB}. \tag{2.16}$$

If the body is freely floating, the buoyancy-to-weight ratio is equal to one, and therefore, if the CG is below CB, the contribution of this term to the restoring moment is positive, while if CG is above CB the contribution is negative. This is an important consideration for FOWTs, since even if the mass of the wind turbine system (rotor plus nacelle plus tower) is usually smaller than the mass of the support structure, the CG of the wind turbine can be very high and push the total CG above the CB. If the body is not freely floating, as for example for a taut or TLP system (see below), the buoyancy-to-weight ratio can be greater than one and therefore, to have $M_{R,CG} > 0$, the CG position has to be lower than the buoyancy-to-weight ratio multiplied by the CB position.

In figure 6, the modified stability triangle concept is represented, taking into account the potential negative contribution of the restoring term due to the CG position, called 'ballast stabilized'. (N.B. In this figure, the negative contribution goes to −25% for the sake of simplicity, but can be higher in modulus.)

(c) Dynamic response

(i) Dynamic response of floating bodies

The six d.f. dynamic response of a free-floating body can be represented by a set of coupled linear second-order differential equations in the complex-frequency domain, based on linear hydrodynamic theory assuming small amplitude displacements as defined, for example, by Faltinsen [29] and Fossen [30]

$$(-\omega^2[\mathbf{M} + \mathbf{A}(\omega)] + \mathbf{j}\omega\mathbf{B}_{\mathrm{hyd}}(\omega) + \mathbf{C})\mathbf{x}(\mathbf{j}\omega) = \boldsymbol{\tau}_{\mathrm{exc}}(\mathbf{j}\omega), \tag{2.17}$$

where $\mathbf{x}$ is the displacement complex vector, $\mathbf{M}$ is the body inertia matrix, $\mathbf{A}(\omega)$ is the hydrodynamic frequency-dependent added mass matrix, $\mathbf{B}_{\mathrm{hyd}}(\omega)$ is the hydrodynamic frequency-dependent damping matrix, $\mathbf{C}$ is the restoring stiffness matrix and $\boldsymbol{\tau}_{\mathrm{exc}}$ is the excitation force. $\boldsymbol{\tau}_{\mathrm{exc}}$ is a combination of all external forces, i.e. wave excitation forces, current forces and wind turbine forces. Wave excitation forces and current forces may be computed through various numerical and semi-empirical approaches [29]. Likewise, wind turbine forces may be computed from a selection of engineering and higher order models [31]. For this set of coupled equations of motion, the eigenvalue problem can be solved to obtain the natural frequencies and modes of the floating body.

(ii) Considerations for floating wind turbines

For the case of a floating wind turbine, the excitation force in (2.17) derives both from incident wave excitations and aerodynamic excitations from the turbine, and the total restoring stiffness matrix consists of hydrostatic stiffness, $\mathbf{C}_{\mathrm{hyd}}$, and mooring restoring stiffness, $\mathbf{C}_{\mathrm{moor}}$, given by

$$\mathbf{C} = \mathbf{C}_{\mathrm{hyd}} + \mathbf{C}_{\mathrm{moor}}. \tag{2.18}$$

The mooring system also contributes to the total system inertia, and in preliminary analyses this contribution is combined with the FOWT inertia matrix. In certain severe operating conditions, the structural and hydrodynamic damping of mooring lines can also have a significant effect on global platform response, although it has not been included here. On this basis, the eigenvalue problem to deduce the six d.f. natural frequencies and coupled vibration modes of the FOWT is given by

$$[[(\mathbf{M} + \bar{\mathbf{A}})^{-1} \cdot (\mathbf{C}_{\mathrm{hyd}} + \mathbf{C}_{\mathrm{moor}})] - \lambda\mathbf{I}]\mathbf{x} = \mathbf{0}. \tag{2.19}$$

The identification of floating wind turbine natural frequencies allows designers to avoid frequency ranges where incident wave forces are significant by appropriately modifying the floating wind turbine characteristics. Equation (2.17) allows for the investigation of the dynamic response of a floating wind turbine for steady-state sinusoidal motions only. The analysis of the transient behaviour of a floating wind turbine would require the time-domain variant of (2.17) that considers free-surface memory effects, as formulated by Cummins [32] and further developed by Oglivie [33]. This time-domain model also allows for the inclusion of the inherent coupling between aerodynamic and hydrodynamic system response, which would otherwise be impractical to consider in frequency-domain models.

3. Comparison of horizontal and vertical axis wind turbine systems

On the basis of the prime principles and considerations illustrated in the previous sections, the aim of the present section is to qualitatively compare a floating offshore VAWT versus a floating offshore HAWT system on the following aspects: static response and stiffness requirements,

Table 1. SPAR and semi-submersible HAWT and VAWT characteristics.

	SPAR		semi-submersible	
	HAWT	VAWT	HAWT	VAWT
$m_{platform}$ (tonnes)	6768.8	7012.2	13342.5	13585.9
$m_{turbine}$ (tonnes)	697.5	454.1	697.5	454.1
m_{total} (tonnes)	7466.3	7466.3	14 040	14 040
$CG_{turbine}$ from MSL (m)	64	24.83	64	24.83
turbine rotational speed (r.p.m.)	12.1	3.7	12.1	3.7
KG (m)	30.08	21.96	10.1	7.44
KB (m)	57.93	57.93	6.82	6.82
draft (m)	120	120	20	20
displacement volume (m^3)	8029	8029	13 917	13 917
$C_{55,total}$ (Nm rad^{-1})	5.31×10^9	5.97×10^9	4.74×10^8	8.461×10^8
$\omega_{n_{33}}$ (rad s^{-1})	0.2217	0.2217	0.3662	0.3662
$\omega_{n_{55}}$ (rad s^{-1})	0.2276	0.2333	0.1502	0.2138

and dynamic response. Furthermore, in order to perform some quantitative considerations, the following VAWT and HAWT FOWT systems will be taken as reference:

— HAWT: NREL offshore 5 MW baseline wind turbine [16].
— VAWT: NOVA 5 MW design [17].

For a description of the geometry of the NOVA VAWT design, refer to [2].

(a) Main characteristics of the reference floating offshore wind turbine systems

Table 1 presents the main characteristics of the floating HAWT and VAWT systems considering as floating support structures a SPAR (OC3-Spar [34]) and semi-submersible (OC4 semi-submersible [35]).

(b) Static response and stiffness requirements comparison

Equation (2.15) estimates what is the minimum stiffness that the FOWT system should provide in order to limit the maximum angle of inclination to θ_{max}. Expanding the terms using (2.5) and (2.12) (always considering the small angle approximation)

$$\underbrace{\rho g I_x}_{A} + \underbrace{F_B \cdot z_{CB} - m \cdot g \cdot z_{CG}}_{B} + \underbrace{C_{55,moor}}_{C} = \frac{\overbrace{F_{env} \cdot (z_{CP} - z_{MLA})}^{D}}{\theta_{max}}. \tag{3.1}$$

(i) Restoring moment due to waterplane area and mooring system

As the aim of the present section is to compare HAWT and VAWT systems, the two SPARs and two semi-submersibles are considered to be identical, having the same displacement, draft and centre of buoyancy (table 1). The mass of the platform is different in order to have the same total mass, and it is achieved using a different amount of ballast. The terms A and C depend only on, respectively, the second moment of the waterplane area (of the support structure) and the mooring configuration, and therefore are considered to be the same for the HAWT and VAWT systems.

Nevertheless, momentarily expanding the analysis to the other d.f., it is worth highlighting some considerations regarding the mooring system. As indicated in §2*a*(iv), the aerodynamic forces produced by HAWTs and VAWTs are markedly different in all six d.f. In general, a VAWT system will generate a substantial yaw torque moment if compared with an HAWT system, and as hydrostatically the platform can generate only a restoring moment in pitch and roll, the counteracting torque yaw moment needs to be generated by the mooring system.

As regards the translational d.f., while heave forces are counteracted by the hydrostatic force on the platform, surge and sway forces can only be counteracted by the mooring system. Therefore, it is necessary to take into account the differences of surge and sway aerodynamic forces in magnitude and trend (approximately constant for the HAWT system, highly oscillatory for the VAWT system).

(ii) Wind turbine mass and CG position

The term B in equation (3.1) is now considered. First of all, it can be noted that as the displacement of the SPAR and semi-submersible systems for the HAWT and VAWT are the same, as well as the position of CB (or KB, the distance between a reference point K, usually the bottom, and CB), the term $F_B \cdot z_{CB}$ is the same for both.

If the complete FOWT system is considered as composed of two systems, the wind turbine (rotor, hub, nacelle, tower) and the floating support structure, the effect of the wind turbine is to raise the CG position, and therefore the restoring moment owing to the term B in equation (3.1) is diminished (de-stabilizing effect). It is simple to derive how much the wind turbine will raise the CG of the total system

$$z_{CG} = \frac{m_{turbine} \cdot z_{CG,turbine} + m_{platform} \cdot z_{CG,platform}}{m_{turbine} + m_{platform}}. \tag{3.2}$$

It can then be seen that the higher the mass of the wind turbine, and the higher the CG position of the wind turbine, the greater the de-stabilizing effect.

Quantitatively, this effect can be seen in table 1. The VAWT has a CG around 25 m above the mean sea level (MSL), whereas for the HAWT system it is 64 m above the MSL. Furthermore, the mass of the NREL 5 MW HAWT system is around 50% higher than the NOVA 5 MW VAWT. This results in a SPAR HAWT FOWT system having an overall CG around 8 m higher than its VAWT counterpart. This leads to a SPAR VAWT system having a restoring stiffness around 12% higher than the SPAR HAWT.

If the semi-submersible is considered, the increase in CG height is lower, as the ratio between the mass of the turbine and the total mass is lower (approx. 3–5% for the semi-submersible, and approx. 6–9% for the SPAR). Nevertheless, for both semi-submersibles the term B in equation (3.1) is negative, i.e. it has a de-stabilizing effect, and as the term $m \cdot g \cdot z_{CG}$ is much higher for the HAWT than for the VAWT, it leads to a final VAWT stiffness in pitch 80% higher than its HAWT counterpart.

(iii) Aerodynamic thrust force magnitude and line of action

If the term D in equation (3.1) is analysed, important differences between a HAWT and a VAWT system can be highlighted. As described earlier, the floating platform considered is the same and also the mooring line action of the mooring systems is considered the same (z_{MLA}). Furthermore, only the aerodynamic component of F_{env}, the aerodynamic thrust T, will be considered. The minimum stiffness required is then proportional to T and the height of the centre of pressure where this aerodynamic force acts (z_{CP}), called the centre of thrust z_{CT}, and the product of the two results in the aerodynamic inclining moment.

VAWTs have the potential to produce the same amount of power with a lower average thrust and/or lower position of the CP, therefore imposing a lower inclining moment on the platform. For the HAWT and VAWT systems considered (figure 2), it can be seen that the thrust force for the HAWT is higher than the mean thrust of the VAWT system considered, but that the VAWT

thrust force varies significantly from approximately 0 to around double the mean value and is much higher than the HAWT thrust force. As regards the CT position, referring to figure 4, it can be seen that due to the substantially different configurations of the HAWT and the VAWT, the VAWT CT height above the wind turbine base is around half of its HAWT counterpart. Another important aspect is that the CT position is approximately constant for HAWT, while for VAWT it depends on the azimuthal position of the wind turbine with respect to the wind direction, and oscillates around the mean position. This occurs since as the individual blades are experiencing different relative velocities and angles of attack through a revolution, the position of the net thrust force varies.

In figure 3, the two inclining moments (note that to be platform independent, these moments are calculated with respect to the CF, but to evaluate the inclining moments for a given platform the arm should be the distance between CT and MLA) are represented. As for the thrust force and centre of pressure, the resultant inclining moment for the VAWT is oscillatory, while it is approximately constant for the HAWT system. Nevertheless, it is important to note that the maximum inclining moment imposed by the VAWT is less than one-third of the moment imposed by the HAWT.

(iv) Considerations about the required stiffness and relative size of the floating support structure

In the present analysis, the same SPARs and semi-submersibles (same displacement, waterplane area, CB position) have been considered for the VAWT and HAWT, in order to have a direct comparison of two systems where only the wind turbines are different.

As a consequence, as the term B in equation (3.1) is higher (for the SPAR or less negative for the semi-submersible systems) for the VAWT system than for the HAWT, the final stiffness in pitch is higher for the VAWT systems than for the HAWT system.

Lower minimum stiffness required. As illustrated in §2*b*(iv), the required minimum stiffness for the VAWT system will be *lower* than the one for the HAWT system, for the same $\theta_{\max}$. This is due to the lower aerodynamic inclining moment.

If the minimum stiffness is lower, then the floating platform for the VAWT can afford to have a smaller second moment of waterplane area, or a less strict limitation on the distance between CG and CB of the system, or the mooring system needs to provide a lower stiffness coefficient, or a combination of these. Whatever be the case, in general, this advantage can be translated into a less costly floating support structure and/or mooring system.

Same minimum stiffness required, but still less costly floating support structure and/or mooring system. The lower position of the CT in figure 4 is mainly due to the novel geometry of the NOVA VAWT. For other VAWT geometries, such as the Darrieus configuration, or the H-type, the CT position will be higher, and the thrust force can be of the same order as the VAWT system. This may lead to an inclining moment imposed by the VAWT similar to the one imposed by the HAWT.

Nonetheless, having the system elements that for HAWT are in the nacelle (gearbox, generator, ancillary systems) at the base of the tower can lead to a lower CG for the VAWT system compared to the HAWT system. Even in this case, despite the fact that the minimum restoring moment is the same for the HAWT and VAWT, the lower CG for the VAWT will mean a higher contribution to the total stiffness from the term B in equation (3.1), and therefore a lower contribution is needed from the terms A and C. Again, this can be potentially translated into a less costly support structure.

(c) Dynamic response comparison

Following the presentation of static characteristics, a dynamic response comparison is presented below. The comparison is performed for wind-only conditions, i.e. there are no incident wave forces acting on the FOWTs and calm water is considered. The wind speeds considered shall be the respective rated wind speeds of the HAWT ($11.4\,\mathrm{m\,s^{-1}}$) and VAWT ($12.9\,\mathrm{m\,s^{-1}}$) systems. The dynamic response was computed using coupled dynamics code FloVAWT, see Collu *et al.* [18], with VAWT aerodynamic forces derived from the Double-Multiple Streamtube blade element

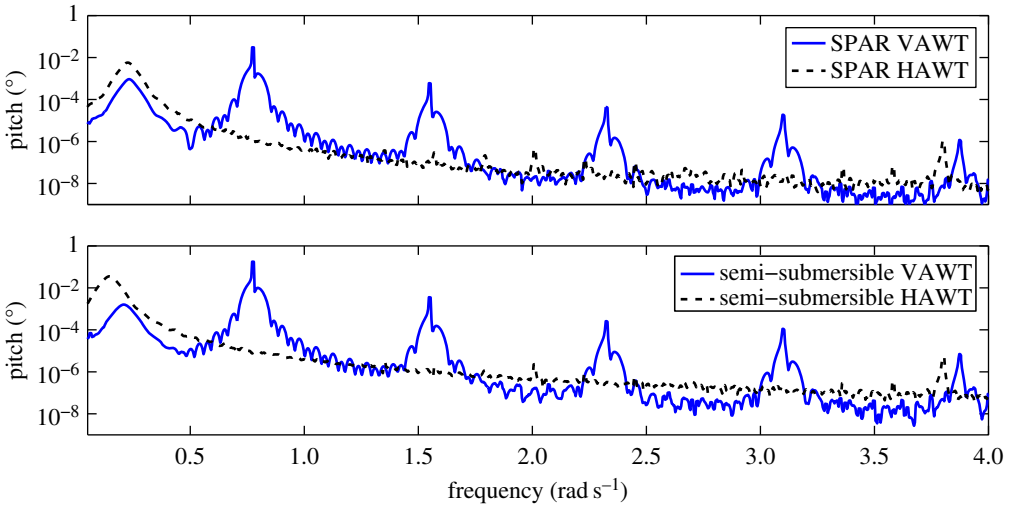

Figure 7. Frequency responses of SPAR and semi-submersible HAWT and VAWT systems pitch motion. (Online version in colour.)

momentum model and HAWT aerodynamic forces derived from the state-of-the-art HAWT blade element momentum code AeroDyn [11]. In this analysis, the blades and tower of both turbines were considered to be rigid only to illustrate the impact of aerodynamic forces on platform motion. Figure 7 presents the frequency responses of the pitch motions of the HAWT and VAWT SPAR and semi-submersible systems. Essentially, figure 7 illustrates the amplitude distribution of platform pitch motion as a function of frequency. This analysis is restricted to pitch only as similar trends are seen in other d.f.

From figure 7, one can immediately identify the natural frequency peaks of all four FOWTs that correspond to the values given in table 1. The dynamic responses of the FOWTs follow similar trends from low frequencies up to around 0.45 rad s^{-1}, from where the impact of oscillatory VAWT aerodynamic forces becomes significant. The frequency at which these aerodynamic forces are greatest is 0.77 rad s^{-1}, equal to the VAWT $n \cdot p$ frequency ([2 blades] × [rotational speed (rad s^{-1})]). Subsequent peaks are also found at integer multiples of this frequency. With regard to the HAWT, the $n \cdot p$ frequency is observed at 3.8 rad s^{-1}. As can be seen at higher frequencies the influence of the HAWT aerodynamic pitch forces is more benign than the influence of the VAWT aerodynamic forces, indicating more fatigue loading on the VAWT system. The excitation of the FOWT in the frequency range 0.5–0.9 rad s^{-1} is of significant importance, as typical sea spectra have the wave energy concentrated in this range. Hence, there is the potential of system excitation from different origins (aerodynamic and hydrodynamic), that may lead to adverse VAWT motion performance, although this has not yet been seen in research.

4. Conclusion

There is currently a lack of research in quantifying the comparison between HAWTs and VAWTs for floating offshore applications. This paper has focused on comparing the static and dynamic responses of floating HAWT and VAWT systems, which is just one of several aspects to be considered. The inherent difference in the interaction between the incident wind and a VAWT and a HAWT results in substantially different aerodynamic forces generated on the support structure. While the thrust force of a HAWT is fairly constant, the VAWT thrust force is highly oscillatory. The same occurs in pitch, but due to the potentially lower line of action of the VAWT thrust, the absolute magnitude of VAWT inclining moment may be significantly lower than of a HAWT. The large yaw moment generated by the VAWT is not seen in the HAWT due

to the nature of turbine operation. These differences are mirrored by the different momentum models adopted.

Starting from prime principles, the static stability of a FOWT was derived, establishing the three main stability mechanisms used by a FOWT and important parameters in identifying the inclining moment of a FOWT. Following this, it was shown that for a given maximum inclination angle criterion the potentially lower inclining moment of a VAWT system would result in a lower required minimum stiffness. Hence, by relaxing this design criterion, a less costly floating support structure can be considered.

An improved floating support structure classification scheme was proposed where the potential negative contribution to the restoring moment of the couple composed by the buoyancy and the weight forces was considered. Also, the mathematical condition to ensure a positive contribution to the restoring moment was derived: the vertical position of the CG of the system should be lower than the vertical position of the CB multiplied by the ratio between the force of buoyancy and weight of the structure. The impact of the mass and the CG of the wind turbine on the static stability of the whole FOWT system is illustrated: the potentially lower wind turbine mass and lower position of the CG of a VAWT was beneficial towards the static stability of the system, as it leads to a lower total FOWT CG position. Hence, the restoring contribution required from the second moment of the waterplane area and the mooring system can be reduced, and this can be translated into a less costly floating support structure.

The dynamic response of a FOWT in the frequency domain was highlighted, and a subsequent case study of two 5 MW HAWT and VAWT illustrated the differences in the dynamic response of the FOWT pitch motion. Owing to the oscillatory nature of VAWT aerodynamic excitation forces, the floating VAWT experiences increased motion in the frequency range surrounding the turbine $n \cdot p$ frequency. For very large VAWTs with slower rotational speeds, this frequency range may significantly overlap with the range of wave excitation forces, which is an important factor to consider in the design of a floating VAWT.

References

1. Collu M, Kolios AJ, Chahardehi A, Brennan FP. 2010 A comparison between the preliminary design studies of a fixed and a floating support structure for a 5 MW offshore wind turbine in the North Sea. In *Int. Conf. on Marine Renewable and Offshore Wind Energy*. London, UK: Royal Institution of Naval Architects.
2. Shires A. 2013 Design action of an offshore vertical axis wind turbine. *Proc. Inst. Civil Eng. Energy* **166**, 7–18. (doi:10.1680/ener.12.00007)
3. Vita L. 2011 Offshore floating vertical axis wind turbines with rotating platform. PhD thesis, Technical University of Denmark.
4. Collu M, Brennan FP, Patel MH. 2012 Conceptual design of a floating support structure for an offshore vertical axis wind turbine: the lessons learnt. *Ships Offsh. Struct.* **9**, 3–21. (doi:10.1080/17445302.2012.698896)
5. Akimoto H, Tanaka K, Uzawa K. 2011 Floating axis wind turbines for offshore power generation—a conceptual study. *Environ. Res. Lett.* **6**, 044017. (doi:10.1088/1748-9326/6/4/044017)
6. Cahay M, Luquiau E, Smadja C, Silvert F. 2011 Use of a vertical wind turbine in an offshore floating wind farm. *Proc. Offsh. Technol. Conf.* **3**, 2064–2076. (doi:10.4043/21705-MS)
7. Betz A. 1926 *Windenergie und Ihre Ausnutzung durch Windüllen*. Göttingen, Germany: Vandenhoeck and Ruprecht.
8. Rankine WJ. 1865 On the mechanical principles of the action of propellers. *Trans. RINA* **6**, 13–30.
9. Froude RE. 1889 On the part played in the operation of propulsion differences in fluid pressure. *Trans RINA* **30**, 390–405.
10. Glauert H. 1935 Airplane propellers. In *Aerodynamic theory* (ed. WF Durand), Div. L, ch. XI, pp. 169–360. Berlin, Germany: Springer.
11. Moriarty PJ, Hansen AC. 2005 AeroDyn theory manual. Technical report no. EL-500-36881. Golden, CO: National Renewable Energy Laboratory.

12. Templin RJ. 1974 Aerodynamic performance theory for the NRC vertical-axis wind turbine. Technical report no. LTR-LA-190. Ottawa, Canada: National Research Council.
13. Wilson RE, Lissaman P. 1974 Applied aerodynamics of wind power machines. Technical report no. PB-238595. Corvallis, OR: Oregon State University.
14. Strickland JH. 1975 The Darrieus turbine: a performance prediction model using multiple streamtubes. Technical report no. SAND75-0431. Albuquerque, NM: Sandia National Laboratories.
15. Paraschiviou I. 2002 *Wind turbine design: emphasis on the Darrieus concept*. Montreal, Canada: Polytechnic International Press.
16. Jonkman JM, Butterfield S, Musial W, Scott G. 2009 Definition of a 5-MW reference wind turbine for offshore system development. Technical report no. TP-500-38060. Golden, CO: National Renewable Energy Laboratory.
17. *NOVA quasi-static rotor design.* 2010 Cranfield, UK: Cranfield University.
18. Collu M, Borg M, Shires A, Rizzo NF, Lupi E. 2014 FloVAWT: further progresses on the development of a coupled model of dynamics for floating offshore VAWTs. In *Proc. 33rd Int. Conf. on Ocean, Onshore and Arctic Engineering, San Francisco, CA, USA, 8–13 June 2014*. (doi:10.1115/OMAE2014-24459)
19. Patel MH. 1989 *Dynamics of offshore structures*. London, UK: Butterworth-Heinemann.
20. Mertens S, van Kuik G, van Bussel G. 2003 Performance of an H-Darrieus in the skewed flow on a roof. *J. Sol. Energy Eng.* **125**, 433–440. (doi:10.1115/1.1629309)
21. Wang K, Hansen MOL, Moan T. In press. Model improvements for evaluating the effect of tower tilting on the aerodynamics of a vertical axis wind turbine. *Wind Energy*. (doi:10.1002/we.1685)
22. Ferreira CJS, van Bussel GJW, van Kuik GAM. 2006 Wind tunnel hotwire measurements, flow visualization and thrust measurement of a VAWT in skew. *J. Sol. Energy Eng.* **128**, 487–497. (doi:10.1115/1.2349550)
23. Zambrano T, MacCready T, Kiceniuk T, Roddier D, Cermelli C. 2006 Dynamic modeling of deepwater offshore wind turbine structures in Gulf of Mexico storm conditions. In *Proc. 25th Int. Conf. on Offshore Mechanics and Arctic Engineering, Hamburg, Germany, 4–9 June 2006*, pp. 629–634. (doi:10.1115/OMAE2006-92029)
24. Wayman EN, Sclavounos PD, Butterfield S, Jonkman J, Musial W. 2006 Coupled dynamic modeling of floating wind turbine systems. In *Proc. Offshore Technology Conf., Houston, TX, USA, 1–4 May 2006*. (doi:10.4043/18287-MS)
25. Van Hees M, Bulder B, Henderson AR, Huijsmans R, Pierik J, Snijders E, Wijnants GH, Wolf MJ. 2002 Study of feasibility of and boundary conditions for a floating offshore wind turbines. Technical report no. 2002-CMC-R43, Drijfwind, The Netherlands.
26. Roddier D, Cermelli C, Aubault A, Weistein A. 2010 WindFloat: a floating foundation for offshore wind turbines. *J. Renew. Sust. Energy* **2**, 033104. (doi:10.1063/1.3435339)
27. Blue H. Floating platform technology for offshore wind energy. See http://www.bluehgroup.com/ (accessed 13 May 2014).
28. Statoil. See http://www.statoil.com/en/technologyinnovation/newenergy/renewablepowerproduction/pages/default.aspx (accessed 13 May 2014).
29. Faltinsen O. 1993 *Sea loads on ships and offshore structures*. Cambridge, UK: Cambridge University Press.
30. Fossen TI. 2011 *Handbook of marine craft hydrodynamics and motion control*. New York, NY: Wiley.
31. Borg M, Shires A, Collu M. 2014 Offshore floating vertical axis wind turbines, dynamics modelling state of the art. Part I: aerodynamics. *Renew. Sust. Energy Rev.* **39**, 1214–1225. (doi:10.1016/j.rser.2014.07.096)
32. Cummins WE. 1962 The impulse response function and ship motions. In *Symp. on Ship Theory*. Hamburg, Germany: Institut fur Schiffbau, Universitat Hamburg.
33. Oglivie T. 1964 Recent progresses towards the understanding and prediction of ship motions. In *Proc. 6th Symp. on Naval Hydrodynamics, Washington, DC*. Arlington, VA: Office of Naval Research.
34. Jonkman JM. 2010 Definition of the floating system for phase IV of OC3. Technical report no. TP-500-47535. Golden, CO: National Renewable Energy Laboratory.
35. Robertson A, Jonkman JM, Masciola M, Song H, Goupee AJ, Coulling AJ, Luan C. 2012 Definition of the semi-submersible floating system for phase II of OC4. Technical report no. TP-5000-60601. Golden, CO: National Renewable Energy Laboratory.